



Research Paper

An improved iterative technique for nonlinear inelastic time history analysis of single degree of freedom (SDOF) elasto-plastic system

Mrs. R. B. Malathy¹, Dr. Govardhan Bhat², Dr. U.K.Dewangan³

¹Research Scholar, Department of Civil Engineering, NIT Raipur, Raipur, India.

¹e-mail: rmalathy.phd2017.ce@nitrr.ac.in

²Assistant Professor, Department of Civil Engineering, NIT Raipur, Raipur, India.

²e-mail: gov.ce@nitrr.ac.in

³Professor, Department of Civil Engineering, NIT Raipur, Raipur, India.

³e-mail: ukdewangan.ce@nitrr.ac.in

Abstract

It is observed that only the primary local mechanism that will form in an earthquake can be differentiated by the pushover analysis and it may not disclose other shortcomings that will be produced when the dynamic attributes of the structure change after the development of the principal mode mechanism. Subsequently, the pushover analysis can be implemented with the limitation that it ought to be supplemented with other assessment systems if higher mode effects are decided to be significant. Hence an effort is made to understand the spread of the plasticity by tracing the control points which essentially represent the state of transition in the elasto plastic model. The Newmark- β strategy for linear system frameworks is extended to nonlinear frameworks by utilizing the Newton-Raphson procedure by addressing the nonlinear state of motions is suggested. In LabVIEW programming, the nonlinear inelastic time-history responses predicted by the proposed program contrast well with those given by the mathematical problem taken for study. Adding to this, the bilinear isotropic hardening model is used to get plastic deformation results in ANSYS 17.0 using finite element method with mesh size as 0.4mm and 0.6mm. These simulations can help to understand how a frame acts when immediate repetitive loads act on the specimen. Furthermore, a small-scale steel frame prototype model was prepared for testing purpose to evaluate the validation of the developed algorithm. The results of the analysis show that the nonlinear iterative approach offers an accurate solution with the experimental work, reflecting both the need for real plastic deformation and the action of catenary stiffness in steel structures. A more practical analysis technique for seismic design can be developed in future by contrasting with the presented program for verification.

Keywords: elasto-plastic system, Newmark β iterative technique, time-history analysis, LabVIEW software, ANSYS 17.0

Received 01 Aug., 2025; Revised 09 Aug., 2025; Accepted 12 Aug., 2025 © The author(s) 2025.

Published with open access at www.questjournals.org

I.Introduction

One of the critical components of nonlinear analysis techniques is the identification of the output point. Extensive research, including the ATC-40 Study [1], suggests nonlinear static strategies based on the Capacity Spectrum System (CSM) in which an equivalent linearization technique is accomplished. The functional limit in this proceeding is compared to the demand for the structure. This methodology dismisses the higher modes commitment in the assessment of target displacement. The Coefficient Method (CM) of FEMA-440[2] depends as another possibility on the strategy of displacement modification in which a few experimentally defined elements are used to modify the reaction of the structure's straight flexible, single-degree-of-freedom (SDOF) model. Compared to FEMA-356[3], equal linearization strategies were enhanced with equivalent period and damping measures with an adjustment to generate a modified acceleration displacement response spectrum (MADRS) matching the capacity spectrum at the Performance Point[4].

In another investigation, an upper-bound pushover examination[7] was constructed in which the contributions of the initial two elastic modes to the invariant load pattern were consolidated through the absolute sum rule. Aydinoglu,[8] outlined Incremental Response Spectrum Analysis (IRSA) using seismic tremor ground motion on a simple two-dimensional structure. This required two basic approximations to be made. To begin with, the customary Response Spectrum Analysis (RSA) method applicable to a linear system is extended to the nonlinear frameworks as an incremental technique which must be implemented at every pushover step in between the two sequential design of the nonlinear framework, or explicitly in between the development of the two consecutive plastic hinges. The second critical assumption was on the assessment of the relative magnitude of the modal displacement increments at each pushover step. The inelastic spectral displacement related to the instantaneous configuration of the nonlinear system was included in the novel scaling methodology proposed for this intent. The practical version of IRSA uses notable equivalent displacement rule for every mode to estimate corresponding inelastic spectral displacement. MPA [9] and IRSA [9] are the solitary techniques that can be viewed as a demand estimation tool, yet in addition as capacity estimation tools. The innovative displacement-based adaptive pushover method is consequently shown to constitute an extremely engaging displacement-based tool for underlying structural evaluation [11]. The most notable approach is the Displacement-based Adaptive Pushover(DAP) expressed by Antonio and Pinho[10], in which a displacement loading is applied and modified at each point by measured properties, softening the structure, thereby increasing its period and also changing the inertial forces due to spectral amplification. Despite the fact that the DAP strategy gives considerable enhancements in assessing the seismic requests when contrasted with conventional force-based pushover strategies, there are still some significant shortcomings. The first is that the equilibrium is not reached by the output and the next problem is that signals are lost during the combination process, eliminating negative quantities contributions. Such extreme deficiencies will play a significant role in reducing the precision of the inter-storey drift profile calculation of the DAP strategy.

A flexible adaptive modal combination (AMC) technique was proposed by Kalkan and Kunnath[11] to decide the objective removal in which a capacity curve is calculated using the energy approach for every mode.

Since the methodology is directed independently for each mode, the primary disadvantage of the MPA system has remained and the conditioning impacts of yielding in one mode isn't considered in others modes. Likewise, the relative capacity curve do not represent the spectra acceleration (load fix) which isn't reliable with structural behavior in inelastic stage. Another part of this strategy is that the loads are applied based on displacement. In order to eliminate the disadvantages of the referenced strategies and integrate the advantage of the various techniques, thus is built an advanced spectra-based multi modal adaptive (MMA) method to overcome the drawbacks[12]. The legitimacy, however, depends on the degree of predicted inelastic action and the number of stories and the measurement of the hinges' plastic rotations. Mehdi Poursha et. suggested another method called the consecutive modal pushover (CMP) that can test higher-mode effects in the pushover investigation of tall structures and improve gauges of the plastic rotations of the hinges. This method subsequently benefits from the principles of multi-stage and single-stage pushover investigations of underlying elements and applications. The accuracy of the adjusted conservative modal pushover (MCMP) strategy has been shown to be more accurate than other seismic demand assessment techniques[13]. Fajfar et al.[14] suggested a technique considering higher mode effects in the plan, which can be used for plan-asymmetric structures. Later, Kreslin M, Fajfar P[15] suggested another approach that takes into account elevation impacts in higher modes. The expanded N2 strategy suggested by Fajfar[16] merged the two ways of dealing with a solitary method that allows the study of medium and tall plan-asymmetric structures. The extended N2 technique, when contrasted with the MPA and MMPA methodology, provides a slightly larger estimate, which is typically conservative compared to the mean values obtained by NRHA[15]. As of late, the MPS system, currently limited to symmetric plan structures, was extended by Reyes and Chopra[17] to unsymmetric plan structures. This technique was applied to single-story unsymmetric-plan structures in the following year by Reyes et al.[18] and contrasted with the ASCE/SEI 7-10 scaling approach for far-field ground movements, which later resulted in the proposal of another version of the MPS system for multi-story asymmetric-plan buildings. The upper-bound (UB) pushover analysis method[8], which was proposed to take into account the effects of higher modes on two-dimensional (2D) high structure frames, underestimates the lower-storey seismic demands. By consolidating the seismic criteria resulting from the upper-bound pushover approach and a classical pushover, Mehdi Poursha[20] made a conscious effort to define the constraint. The results explain that the all-inclusive approach will interpret the inelastic seismic requests of unsymmetric-plan tall structures to a realistic precision. In order to generate higher modes, the same author suggested a single run multi-mode pushover (SMP) system to take account of the seismic request requirements of tall structure frames. Only a single invariant lateral force distribution is necessary along these lines. The proposed strategy also has the advantage that spectral pseudo-acceleration that was integrated into the distribution of lateral force[21]. A multi-mode adaptive force-based pushover (AFMP)[22], a non-adaptive displacement-based (NADP) procedure[23] and an Adaptive Capacity Spectrum System (ACSM)[24] based on the Inelastic Demand Response Spectra (IDRS) were implemented to

reflect the impact of higher modes in the assessment of seismic requests of tall structures. The strategy uses some single-run traditional and improved pushover analysis.

It is therefore well concluded that the interaction between modes in the nonlinear range can not be expressed by multi-run techniques. The research concluded that the arrangement of control points at the end of each loading and unloading branch is deficient. In addition, a few issues of the incremental iterative nonlinear investigation of framed systems, including the experience of the post-buckling response, should be solved from hypothetical perspectives. It can also be assumed that we should not limit ourselves only to the determination of the component or primary stiffness matrices in assessing previous works on nonlinear examination. It is not extraordinary that papers centered primarily on the derivative of the same, with little touch on the different elements of the incremental-iterative method, on the geometric nonlinear investigation of structures. The probability of simplification of the plastic hinge method in the formulation of structural elements in the detailing of primary components for inelastic investigation [22] cannot be prohibited. It is shown that the plastic deformation generated by the behavior of the member can be represented by a plastic hinge at the end of the member concerned, while the majority of the hinge remains elastic [27]. In order to investigate the nonlinear inelastic behavior of 3D steel frames representing lateral-torsional buckling, An improved fiber plastic hinge system was introduced by Nguyen and Kim[28], using mathematical stiffness and stability capacities to account for the second-order effects. The plastic hinge method has the advantage of being applied to actual design at a lower cost, as there is no reasonable reason for tedious time-consuming discretization and numerical integration to be performed as required by the technique of the plastic zone. It also has the accompanying problem, however, that the impact of strain hardening, residual stress and elastic discharge cannot be precisely included in the model of analysis [27]. The distributed plasticity method developed by P.C.Nguyen et al. for nonlinear dynamic analysis is revised based on the Newmark β iterative strategy in the context of its SDOF nonlinear structure applications [27]. A mathematical system is proposed for carrying out the second-order inelastic time-history study of planar steel frames subject to dynamic loadings and seismic tremor excitations. It uses an elastic model with strain hardening of entirely plastic material. Using the Rayleigh-Ritz technology and the theory of stationary potential energy, the tangent stiffness matrix of the nonlinear beam-column component is easily checked for the effects of geometric nonlinearity and gradual yield of the material. The orientation of the strain-hardening and elastic neutral axis is easily seen during the process, as in the tangent stiffness matrix, due to the yield of such fibers is in the cross-segment [29]. In LabVIEW programming, a computer program using the Newmark- β method is built to acquire convergent solutions with respect to the nonlinear problem. In order to quantify displacement and force increases, this code is written for each control point to model loading and unloading states as the control point focuses essentially on a state of transitions under earthquake excitations. Only the SDOF elasto-plastic structure will be of interest in this paper. In addition, the effects of nonlinear inelastic reactions are contrasted with those of mathematical problems, demonstrating the accuracy of the nonlinear iterative technique proposed. The proposed technique reflects all the significant limits, such as the degree of gravity loads, the plastic rotation specifications in steel individuals, the post elastic stiffness and the catenary stiffness behavior in the structure. Furthermore, it overcomes the challenges of different formulations available in previous literature that usually disregard one of these iterativity constraints.

II. Analysis Method

2.1 Limitations and opportunities of iterative technique

In the present work, the modified rather than the full Newton-Raphson iteration method is adopted due to the former's efficiency in second-order plastic-zone analysis of steel frames. In any nonlinear problem, the nonlinearity can be restricted to the ends of the member within a certain length. It requires monitoring of stiffness changes in a compound at all such locations. The equation of motion becomes nonlinear if the structure has nonlinear terms either in inertia or in damping or in stiffness or in some form of combination of them. The equation of motion at time t is given as:

$$m\ddot{x}(t) + c\dot{x}(t) + f(x) = p(t)$$

or, at i^{th} step

$$m\ddot{x}_i(t) + c\dot{x}_i(t) + f(x_i) = p_i$$

And at $i+1$ step

$$m\ddot{x}_{i+1}(t) + c\dot{x}_{i+1}(t) + f(x_{i+1}) = p_{i+1}$$

The change over these two steps is

$$m\Delta\ddot{x}_i + c\Delta\dot{x}_i + \Delta f_i = \Delta p_i$$

Where, $\Delta f_i = f(x_{i+1}) - f(x_i) = (k_i)_T \Delta x_i$

The force $f(x)$ represents resisting force which depends upon the member stiffness and deformations. The tangent stiffness is a function of displacement and would not be constant in a nonlinear problem. Within any time step, increments in node displacements are computed and hence there are increments in member deformation. Increments in the component forces corresponding to these deformation increments should be

determined, taking into account the change in the stiffness of the element. As the new state of force and deformation in each variable is calculated, this is the state determination step of the calculation. The relationship between element force and deformation can be represented by piecewise linear curve as shown in the (Fig.2.1a).

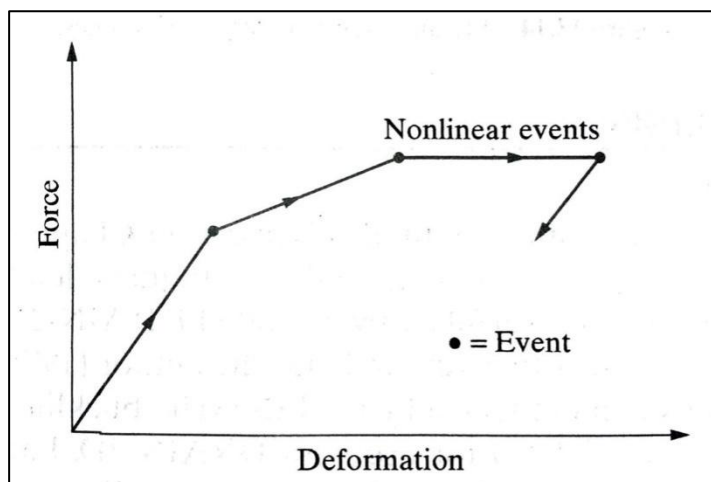


Figure.2.1a Definition of event

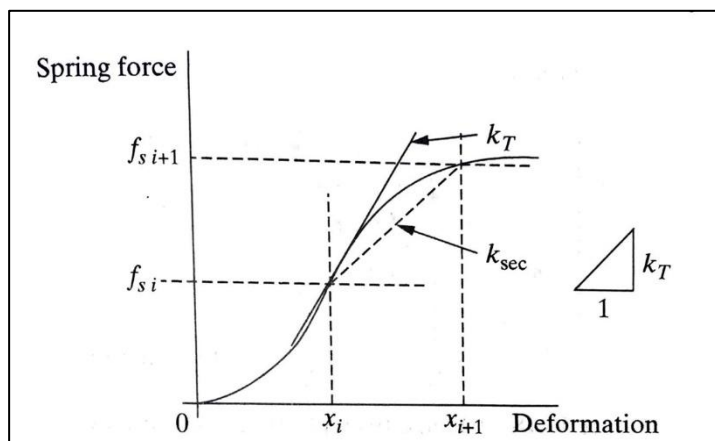


Figure 2.1b Tangent and secant stiffness

Each slope shift corresponds to a stiffness change at a new point or unloading at a point previously yielded and will be called a case. In general, multiple events can occur within a single time phase for any variable. The element deformation is typically more meaningful for inelastic structures than the element force because deformation provides a clear indication of the need for ductility on the structure. There is a need to keep track of displacement and velocity at each time increment. A zero or negative velocity indicates a change in direction of loading or unloading.

The tangent stiffness k_T and secant stiffness k_{sec} at any instant 't' are shown in the (Fig. 2.1b). in the step-by-step numerical integration for a nonlinear problem, three situations are encountered as discussed earlier and shown in the various hysteresis models:

1. Change from elastic to plastic state (loading)
2. Continue in the plastic state (loading)
3. Change from plastic to elastic state (unloading)

Change of state from elastic to plastic At the beginning of a time step, say at point 'a', the tangent stiffness at point 'a' is assumed and the numerical analysis will lead to point 'b' as shown in the fig. 2.1c. It should have led to point b' which is the correct answer. Obviously, a tangent stiffness will never lead to the correct point b'. the point b' is unknown at this stage and can be located by iteration.

$$\Delta f_i - (k_i)_T \Delta x_i = \Delta R_i$$

$$\Delta f_i = \text{true resisting force}$$

$$(k_i)_T \Delta x_i = \text{approximate resisting force based on tangent stiffness}$$

ΔR_i =residual or unbalanced resisting force

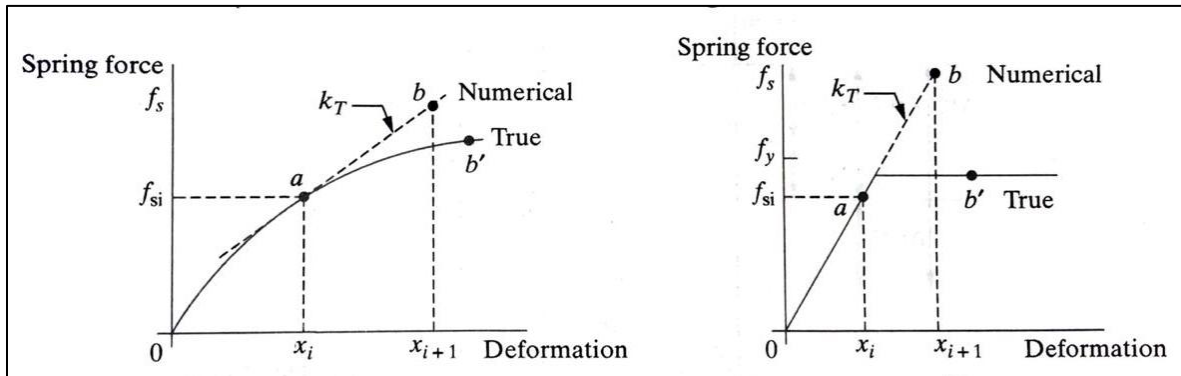


Figure 2.1c and 2.1d Change of elastic to plastic state

Continue in plastic state

Upon further loading, the member may continue to plastify, that there will be no increase in its resistance but it will keep on deforming as shown in the fig.2.1d.

Change of state from plastic to elastic

At the beginning of a time step, say at point 'a', the stiffness at point 'a' is assumed and the numerical analysis will lead to point 'b' as shown in the fig 2.1e. In case the velocity at point 'b' is negative or zero, it means the system is now under unloading. Upon unloading from point b, the analysis will lead to point 'c'. Both the points, b and c are incorrect. The velocity at the beginning of the time step at point 'a' was positive and somewhere in between 'a' and 'b', the velocity has become zero, say at point b' . It means the true unloading will begin at point b' and should lead to point c' which will be the true behaviour. Point b' can be located either by iteration or by choosing a very small time step between points 'a' and 'b'.

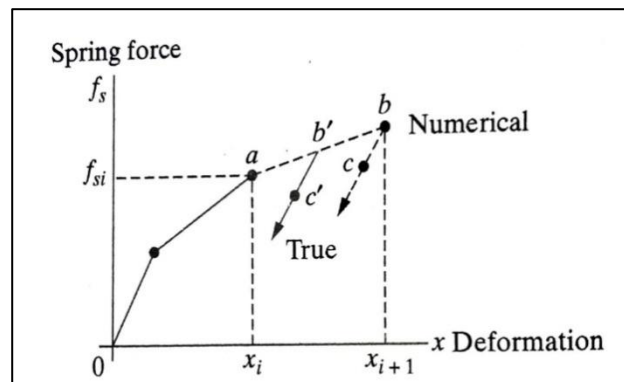


Figure 2.1e Change from plastic to elastic state

There are different numerical techniques for the solution of nonlinear problems depending upon the complexities involved in the nonlinear behaviour.

2.1.1 Newmark β Method: With Iterations

The Newmark β method for linear systems can be extended to nonlinear systems by making use of the Newton-Raphson technique. The salient features of this step-by-step method for nonlinear systems can be explained with the help of a force-deformation curve as shown in Fig. 3.

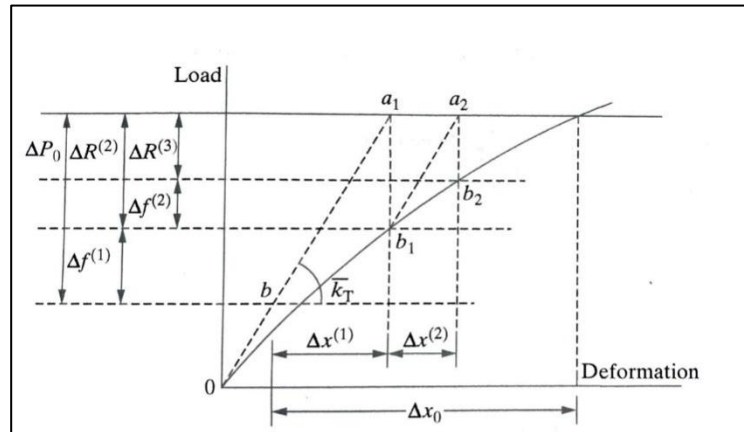


Figure 2.1.1a Modified Newton Raphson

$$\bar{k} = \frac{\Delta \bar{p}}{\Delta x_i}$$

where

$$\bar{k} = k + \frac{\gamma}{\beta \Delta t} c + \frac{1}{\beta (\Delta t)^2} m$$

and

$$\Delta \bar{p}_i = \Delta p_i + \left(\frac{1}{\beta \Delta t} m + \frac{\gamma}{\beta} c \right) x_i + \left[\frac{1}{2\beta} m + \Delta t \left(\frac{\gamma}{2\beta} - 1 \right) c \right] \ddot{x}_i$$

In the nonlinear analysis, tangent stiffness k_T is used instead of k

$$\bar{k} = k_T + \frac{\gamma}{\beta \Delta t} c + \frac{1}{\beta (\Delta t)^2} m$$

where $(k_i)_T$ = tangent stiffness which is a function of force-displacement relation of a member.

In static load case, there are no mass and damping terms. The nonlinearity is caused due to stiffness of k_T alone. Therefore, its effect is quite severe. In dynamic systems, the coefficients of mass and damping terms in \bar{k} , $\frac{1}{\beta (\Delta t)^2}$ and $\frac{\gamma}{\beta \Delta t}$ are much larger than k_T for usual values of β and Δt . Therefore, the severity of nonlinearity is reduced. In fig 2.1.1a, corresponding to a force Δp_0 , the correct deflection is x_0 . For a force Δp_0 , the linear analysis will give a deflection Δx_1 corresponding to point b_1 which is obviously incorrect.

$$\bar{k}_T \Delta x_0 = \Delta p_0$$

This will lead to a deflection $\Delta x^{(1)}$ instead of Δx_0 . $\Delta x^{(1)}$ is the first approximation to the true Δx_0 . Corresponding to $\Delta x^{(1)}$, the true force is $\Delta f^{(1)}$ which is less than Δp_0 . The residual or unbalanced force is defined by

$$\Delta R^{(2)} = \Delta p_0 - \Delta f^{(1)}$$

The additional displacement due to this residual or unbalanced force is given as

$$\bar{k}_T \Delta x^{(2)} = \Delta R^{(2)} = \Delta p_0 - \Delta f^{(1)}$$

This additional displacement is used to find a new value of the unbalanced force, and the process is continued until the solution has converged. This iterative process is referred to as the *modified Newton-Raphson* method because the same initial stiffness is used throughout.

The algorithm can be written as follows:

Phase 1: For the given system parameters, initialize the Newmark's constants a_0 to a_7 and compute the initial acceleration \ddot{x}_0 .

Phase 2: For each time ($i=0,1,2,3,\dots$) Compute \bar{k}_{Ti} and $\Delta \bar{p}_i$

(a) Set $\Delta R^{(i)} = \Delta \bar{p}_i$ and $x_{i+1}^{(0)} = x_i$ to begin the iteration.

(b) Carry out Newton-Raphson iterations within a time step:

(c) Solve the equilibrium equation for deflection Δx :

$$\bar{k}_T \Delta x^{(j)} = \Delta R^{(j)}$$

$$\Delta f^{(j)} = f_s^{(j)} - f_s^{(j-1)} + (\bar{k}_T - k_T) \Delta x^{(j)}$$

$$\Delta R^{(j+1)} = \Delta R^{(j)} - \Delta f^{(j)}$$

$$x_{i+1}^{(j)} = x_{i+1}^{(j-1)} + \Delta x^{(j)} \quad j = 1, 2, 3, \dots$$

where, the term $(\bar{k}_T - k_T)$ corresponds to the contribution of mass and damping terms in the equivalent stiffness.

(d) The acceleration increment and velocity increment can be estimated from the equations developed earlier for the Newmark's method.

$$\Delta \ddot{x}_i = \frac{1}{\beta(\Delta t)^2} \Delta x_i - \frac{1}{\beta \Delta t} \dot{x}_i - \frac{1}{2\beta} \ddot{x}_i$$

$$\Delta \dot{x}_i = \frac{\gamma}{\beta \Delta t} \Delta x_i - \frac{\gamma}{\beta} \dot{x}_i + \Delta t \left(1 - \frac{\gamma}{2\beta}\right) \ddot{x}_i$$

(e) Finally, when the iterative process has converged, the total incremental displacement is given by, $\Delta x_0 = \Delta x^{(1)} + \Delta x^{(2)} + \Delta x^{(3)} + \dots$

In this procedure, for all iterations, an initial stiffness matrix is used. The stiffness matrix triangularization operation is carried out only once and the convergence is very slow in this iterative scheme. Yet, in certain problems involving mild nonlinearities, this proves less expensive on the whole.

Convergence Criteria In any iterative scheme, there has to be a convergence criterion to stop the process. Either $\Delta R^{(j)}$ or $\Delta x^{(j)}$ may be chosen smaller than a limiting value. Another option is to check the ratio $\Delta R^{(j)} / \Delta \bar{p}$ or $\Delta x^{(j)} / \Delta x$ to be sufficiently small. The total increment Δx will not be known till the iteration process is complete, therefore, $\sum \Delta x^{(j)}$ may be used in place of Δx .

A better convergence is achieved by using the *current tangent stiffness* in place of the *initial stiffness*. It requires greater computational efforts because of the assembly of tangent stiffness matrix and, therefore, triangularization of such a matrix for each iteration. This iterative scheme is known as the *Newton-Raphson* method.

III. Numerical studies and discussion

In order to evaluate the iterative technique in identifying the state of transition, we have considered a variety of problems as numerical examples. The examples considered are either widely investigated by earlier researchers or the problems which are commonly encountered. Apart from the numerically simulated examples, we have also considered the experimental results of the benchmark problems available online to evaluate the efficiency of the program proposed for the iterative technique. It is verified for accuracy and efficiency by the comparison of the prediction with those generated for nonlinear time history analysis using SDOF elasto-plastic system.

3.1 Numerical example for validation

The numerical example is formulated to demonstrate the effectiveness of the proposed nonlinear iterative Newmark β method by comparing with the nonlinear non iterative Newmark β method.

A SDOF elasto-plastic system with mass 2.5kg, tangent stiffness 250N/m, viscous damping 5% and yield strength 5N was chosen. It was subjected to a dynamic loading and its response at 2.20sec and 2.34sec are shown in the table 1. The step size considered was 0.02 sec and load increment was 0.1 sec.

Table 1

Time	Displacement	Velocity	Acceleration	Spring Force	Load
Sec	m	m/s	m/s ²	N	N
2.20	0.01825	0.2205	-1.8455	4.5625	0.5
2.34	0.0346	0.01470	-3.3147	5	-3.25

The response at 2.22 sec and 2.36 sec are calculated using iterative Newmark β method. The results obtained at the time step 2.20 sec and 2.34sec from the text are shown below in table 2 and 3.

Table 2

At time step 2.20 sec	
Total displacement	0.02228m
Velocity at the end of a step in time	-0.0379m/s
Acceleration at the end of a step in time	-1.9426m/s ²

Table 3

At time step 2.34 sec	
Total displacement	0.03424m
Velocity at the end of a step in time	-0.05083m/s
Acceleration at the end of a step in time	-3.1583m/s ²

Programming in LabVIEW

Based on the above-mentioned nonlinear iterative Newmark β formulations, a computer program written in LabVIEW is generated to predict the change in the state of the SDOF elasto-plastic system subject to the above-mentioned static load. The effect of the initial residual stress is also analyzed and seen in the

program. For these cases, the coefficient $\beta = 1/4$ and $\gamma = 1/2$ is used in the dynamic analysis. The block diagrams are formulated and the solutions are shown in the front panel.

Algorithm:

Step 1: Calculate the natural frequency and \bar{k} .

Step 2: Calculate the effective load increment, velocity increment and spring force.

Step 3: Calculate the change of state.

Step 4: The plastic deformation in the element at various time step is calculated.

Step 5: Calculate the total displacement, velocity and acceleration at the end of the each time step.

The solutions for time step 2.20sec are displayed on the front panel is shown in fig 3.1a and fig 3.1b

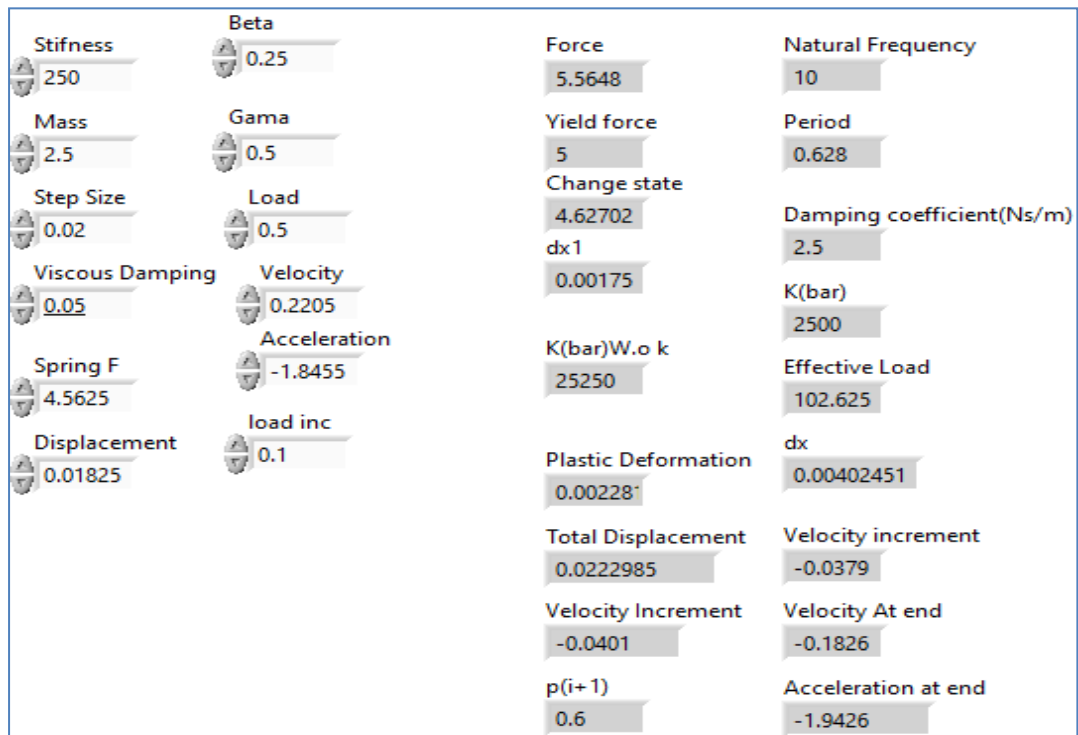


Figure 3.1a

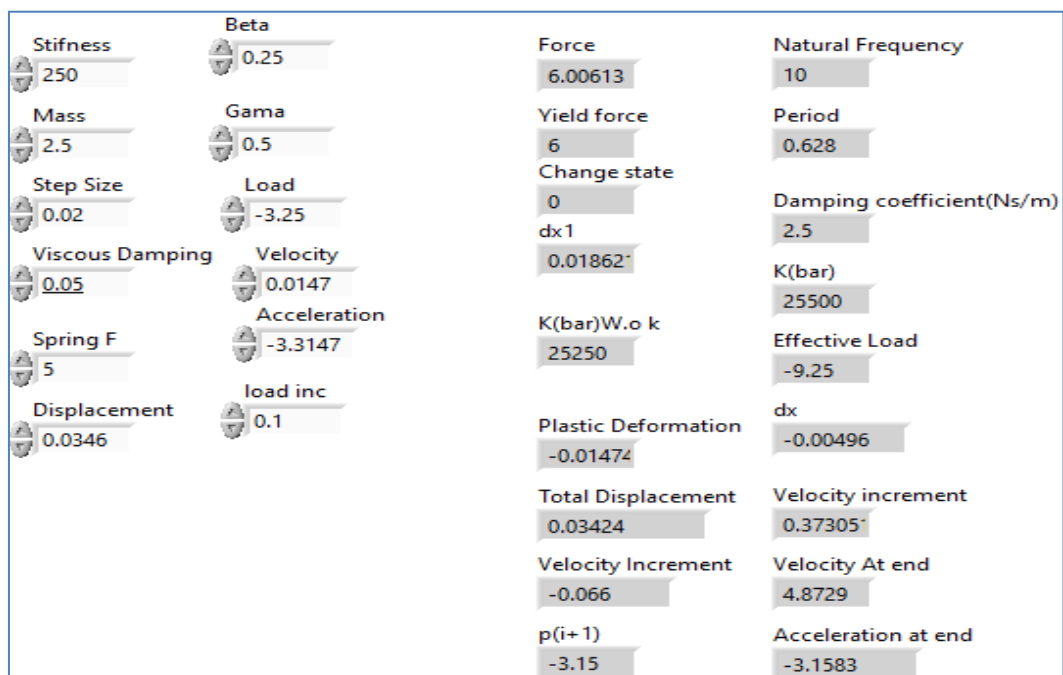


Figure.3.1b(mistake: its not velocity increment in the program)

After performing the analysis, it can be clearly seen that a strong agreement of values of the displacement, velocity and acceleration is generated by LabVIEW and the iterative technique. Hence the programming can be further established for time history analysis of structure to identify the change of state in it.

Test model and experimental results

A prototype three-bay and three-story structure(PS) with 3.6m height and 1.84×2.04 m plan is given in the figure. It is designed according to Indian codes for a Peak Ground Acceleration (PGA) of 0.34 g (here g is the acceleration of gravity). The PS is braced in one direction with v-type braces such that the system is weak in y-axis and strong along x-axis.

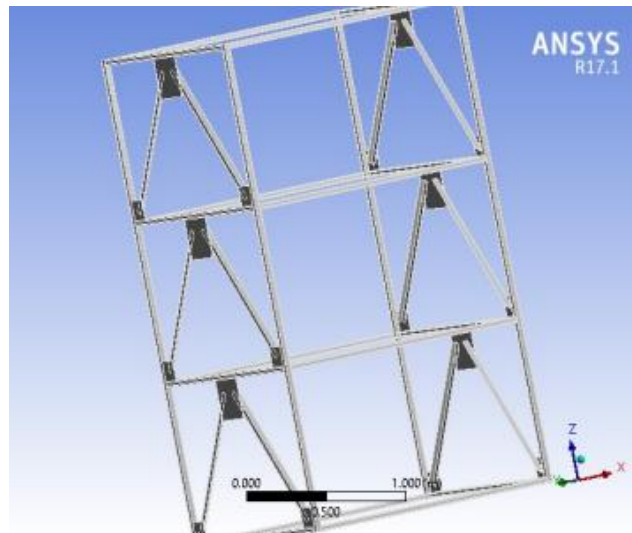
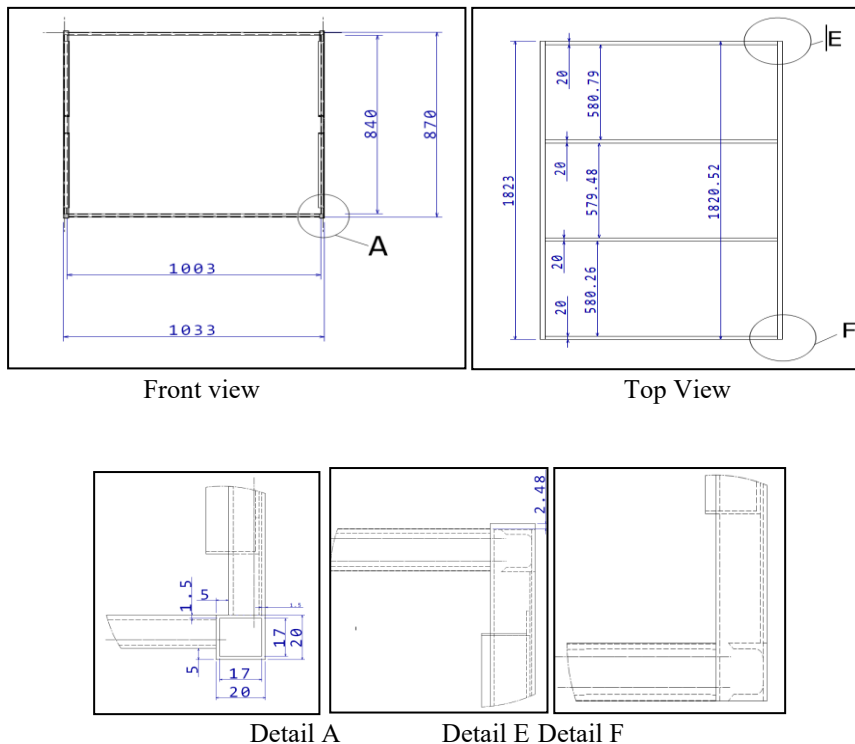


Fig. Stick model of the experimental model



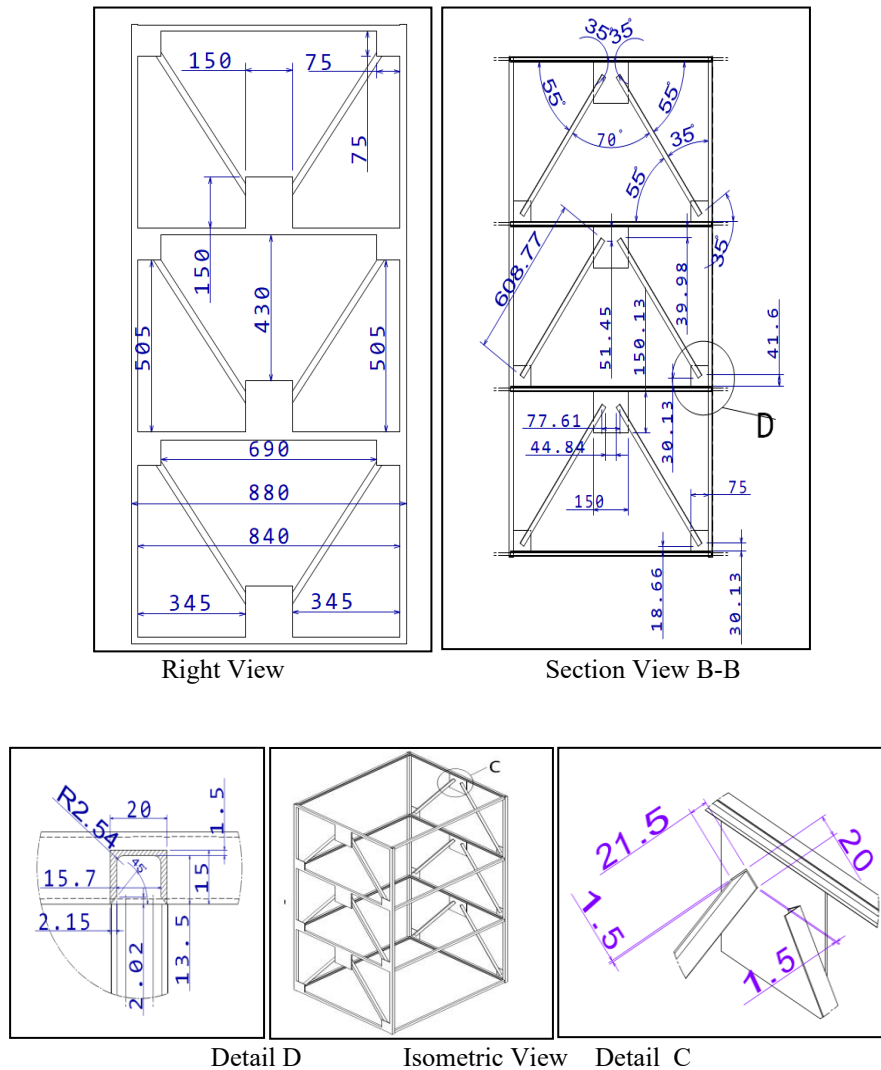


Fig: Section Properties of the experimental structure

Description of the test models

From the prototype structure, a reduced-scale test model satisfying the similitude laws was designed. The test model was derived applying the following scaling factors for geometry, acceleration and stress, respectively: $\lambda_l = 1/2$, $\lambda_a = 1$ and $\lambda_\sigma = 1$. A three storey structure was built in the Structural Engineering Laboratory at the National Institute of Technology, Raipur. Tables 1a, 1b shows the geometry details of the scaled test model. The detailing of the column braces and girder are mentioned in Fig 1a.. The steel girders of 20x15 mm with a thickness of 1.5 mm is provided to prevent punching shear failure. The braces of 20x20mm with a thickness of 1.5mm are provided to withstand the lateral loads. The column is 20x20mm with a thickness of 1.5mm deep. The dimensions of the plate were 150x150x1.5mm and 75x75x1.5mm. The average yield stress, f_s , of the reinforcing steel was 2.5e+008 MPa. The structure tested in this study is idealized as a SDOF system.

Table 1a Structural detail of the prototype structure

Bounding Box	
Length X	1.033 m
Length Y	0.88 m
Length Z	1.823 m
Properties	
Volume	3.0405e-003 m ³

Mass	23.868 kg
Scale Factor Value	1.
Statistics	
Bodies	1
Active Bodies	1
Nodes	26941
Elements	13893
Mesh Metric	None
Basic Geometry Options	
Solid Bodies	Yes
Surface Bodies	Yes
Line Bodies	No
Parameters	Independent

Table 1b: Structural detail of the prototype structure

Thermal Strain Effects	Yes
Bounding Box	
Length X	1.033 m
Length Y	0.88 m
Length Z	1.823 m
Properties	
Volume	3.0405e-003 m ³
Mass	23.868 kg
Centroid X	-0.519 m
Centroid Y	3.5766e-009 m
Centroid Z	-0.89277 m
Moment of Inertia Ip1	11.231 kg·m ²
Moment of Inertia Ip2	13.635 kg·m ²

Moment of Inertia I_p	8.0884 kg·m ²
Statistics	
Nodes	26941
Elements	13893
Mesh Metric	None

(PHOTO OF THE EXPERIMENTAL SETUP)

Structural Steel > Constants

Density	7850 kg m ⁻³
Coefficient of Thermal Expansion	1.2e-005 C ⁻¹
Specific Heat	434 J kg ⁻¹ C ⁻¹
Thermal Conductivity	60.5 W m ⁻¹ C ⁻¹
Resistivity	1.7e-007 ohm m

Structural Steel > Compressive Yield Strength

Compressive Yield Strength Pa
2.5e+008

Structural Steel > Tensile Yield Strength

Tensile Yield Strength Pa
2.5e+008

Structural Steel > Tensile Ultimate Strength

Tensile Ultimate Strength Pa
4.6e+008

Structural Steel > Isotropic Secant Coefficient of Thermal Expansion

Zero-Thermal-Strain Reference Temperature C
22

Structural Steel > Strain-Life Parameters

SCoefficient Strength	Strength Exponent	Ductility Coefficient	Ductility Exponent	Cyclic Strength Coef Cyclic Strength	Cyclic Strain Hardening Exponent
-----------------------	-------------------	-----------------------	--------------------	--------------------------------------	----------------------------------

Coefficient Pa				Coefficient Pa	
9.2e+008	-0.106	0.213	-0.47	1.e+009	0.2

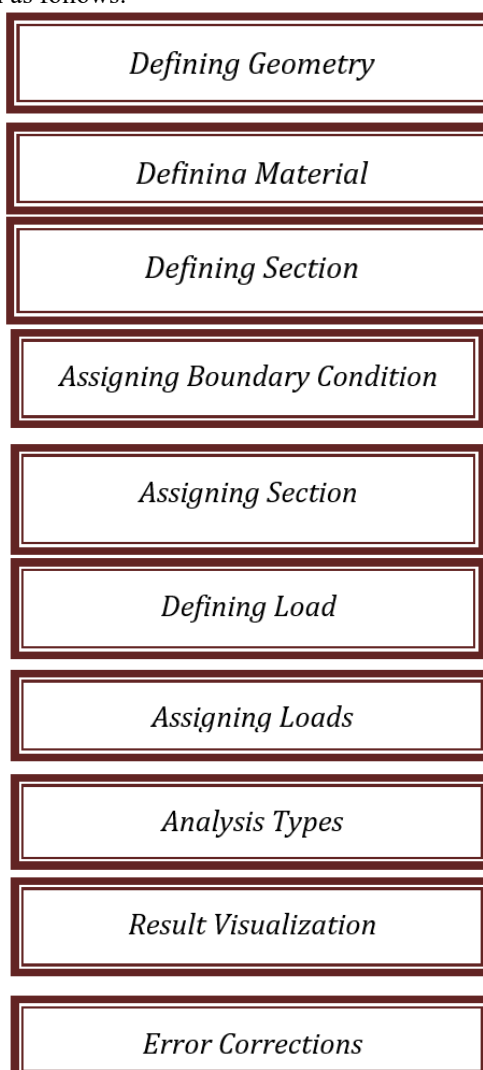
Structural Steel > Isotropic Elasticity

	Young's Modulus Pa Shear Modulus Pa	Poisson's Ratio	Bulk Modulus Pa	Shear Modulus Pa
	2.e+011	0.3	1.6667e+011	7.6923e+010

Structural Steel > Isotropic Relative Permeability

Relative Permeability
10000

The modeling Hierarchy is given as follows:



The dynamic tests were carried out on the uniaxial 2×2m shake table of the National Institute of Technology. Fig. 1 shows the modeling hierarchy that is implemented for carrying out the experiment. The test models were bolted to the shaking table as seen in Figs. 4 and 5. In order to satisfy the similitude laws between prototype and test model, additional mass was added to the top of the frame; the total mass including the steel blocks was $M = 7.39 \text{ Ns}^2/\text{mm}$. The natural vibration of the reduced-scale structure at each step is more than the prototype structure; the upper limit of the working frequency of the designed shaking table is kept less than 1.5 Hz, and the lower limit more than 0.305 Hz. The accuracy in frequency is maintained up to 0.01 Hz. The uniaxial shake table has a single-board Arduino Nano microcontroller with digital and analog input/output (I/O) pins making the serial communication interfacing possible. The frequency from the VFD is given to the three-phase induction motor. The motor moves in the clockwise direction when the positive frequency is applied specifically.

A generalized application in LabVIEW was designed to process the real-time data in the form of serial data using serial communication via NIVISA. The Kalman filter was used to model the motion control of the system. A new adaptive algorithm was created using Kalman filter to provide harmonic data. In order to render the discretization

error in Kalman filter using efficient high-pass filter, a new Kalman filter combined with Butterworth filter is proposed. Thus, it measures control system dynamics directly and modifies the control compensation accordingly in real time, making it possible to adapt to changing system dynamics.

The model was tested by applying 0.305Hz to 1.5Hz to the shake table. Data was continuously collected by as data acquisition system using a sampling rate of 0.1Hz. During each seismic simulation, displacements, strains and accelerations were acquired simultaneously. The Figure 6a, b show the time history of displacement and is used as ground excitation in dynamic analysis. Their peak ground accelerations and timesteps are listed in Table 1. Several numerical examples are presented and discussed to verify the accuracy and efficiency of the proposed program in predicting the response of semi-rigid steel frame structures subjected to dynamic loadings. For verification purposes, the predictions obtained from the proposed program are compared with available results reported in the literature, and those generated by ANSYS. It should be noted that SAP2000 did not provide a semi-rigid element accounting for nonlinear effects of beam-to-column connection, whereas the proposed element can consider these effects.

The frame model is instrumented with the following sensors:

- (a) MPU motion sensor measured the relative horizontal displacement, v , between the shake table and the frame in the direction of the dynamic loading;
- (b) An accelerometer labelled “I-TEDS Accelerometer” with the sensitivity rate of 114.2 mV/g shown in Fig. 4 was fixed to the shake table to measure the absolute table acceleration in the direction of the loading.
- (c) Strain gauges were attached to top and bottom sides of the columns as shown in Fig. 4.
- (d) Two sensors each on the diagonal braces measured the axial deformation in it.

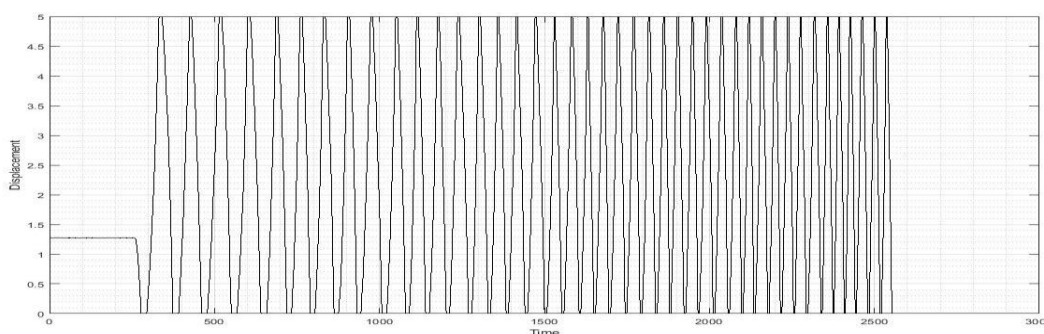


Figure: Displacement time history

IV. Results and discussion

4.1 Nonlinear analysis of the investigated model

The accuracy of the proposed procedure is evaluated by performing nonlinear time stepping technique. Three cases are distinguished: 1) elastic stage; 2) plastic stage without catenary stiffening effect and 3) plastic state with catenary stiffening effect. The elastic case limits the stress value below the first yield point, which is said to be the elastic strain range. The range beyond is the ultimate strain range. The ductility ratio defines the proportion between the ultimate to elastic strain. It can be clearly noticed that the steel has enough capacity which is not utilized in elastic design. Thus, it can be clearly concluded that the elastic design principles do not utilize the material strength beyond the yield value. The critical issue in this is the material

strength beyond yield value is very high, which is referred as “ reserved strength” in literature yields gain and also loss. The postive aspect that we encounter is sufficient load carrying capacity and the loss is permanent plastic deformation. Thus we can arrive at a conclusion that the first yield point should not decided as the steel strength as it has enormous strength beyond the first yield point.Hence we need to take the advantage of the inelastic behaviour in design. The great advantage in the transition of elastic to plastic design to use the resreved strength is ductility. The ductilty redistributes the moment from highly streessed section to the adjacently located high stressed section of statically indeterminate structure. This mechanism is studied by applying nonlinear time hstory analysis to understand the redistribution of moments from highly stressed cross section to the successive section.

4.2 Selection of ground motion data for analysis

The selection of representative input ground motions (IGMs) is important for a proper nonlinear response time history analysis (NLRHA) of modern structures[31]. ASCE/SEI 7–10 [32] has clearly stated that ” If seven or more pairs of ground motions are used for the response-history analysis, the average value of the response parameter of interest is permitted to be used for design. If fewer than seven pairs of ground motions are used for analysis, the maximum value of the response parameter of interest shall be used for design.” Hence a match of earthquake accelerograms to specific target response spectrum using the wavelet algorithm is done using SeismoMatch software. The mean matched spectrum with a predefined tolerance in maximu misfit is performed using a group of seven randomly selected IGMs.The details of the selected earthquake acceleograms data from PEER Strong Motion database are listed in the table 4.

Table 4

Sl.no	Earthquake	Year of Occurance	Recording Station	Timestep(s)	Frequency range
1	The Chi-Chi (Taiwan)	20 th September, 1999	TCU045	0.01	0.02-50.0 Hz
2	The Kobe (Japan)	16 th January, 1995	KAKOGAWA	0.01	0.1-unknown
3	The Kocaeli (Turkey)	17 th August, 1999	YARIMCA	0.01	0.07-50.0 Hz
4	Landers, The Landers (USA)	28 th June, 1992	SCE STATION 24	0.01	0.08-60.0 Hz
5	The Loma Prieta (USA)	18 th October, 1989	CDMG STATION 47381	0.01	0.1-40.0 Hz
6	The Trinidad (USA)	24 th August, 1983	CDMG STATION 1498	0.01	0.15-30.0 Hz
7	The Valley of Imperial (USA)	15 th October, 1979	USGS STATION 5115	0.01	0.1-40.0 Hz

The basic spectral matching of time histories using SeismoMatch software closely matched the original earthquake accelerogram to the target response spectrum of IS 1893 2016. The unmatched and matched earthquake accelerogram graph is shown in the fig 4.2a and fig 4.2b respectively.

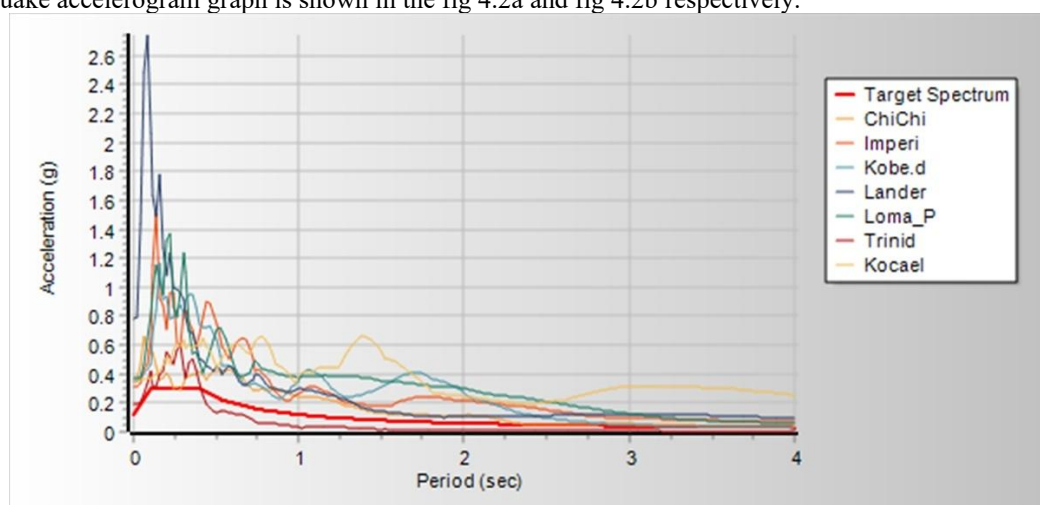


Fig.4.2a Original earthquake acceleogram values with resopnse spectrum

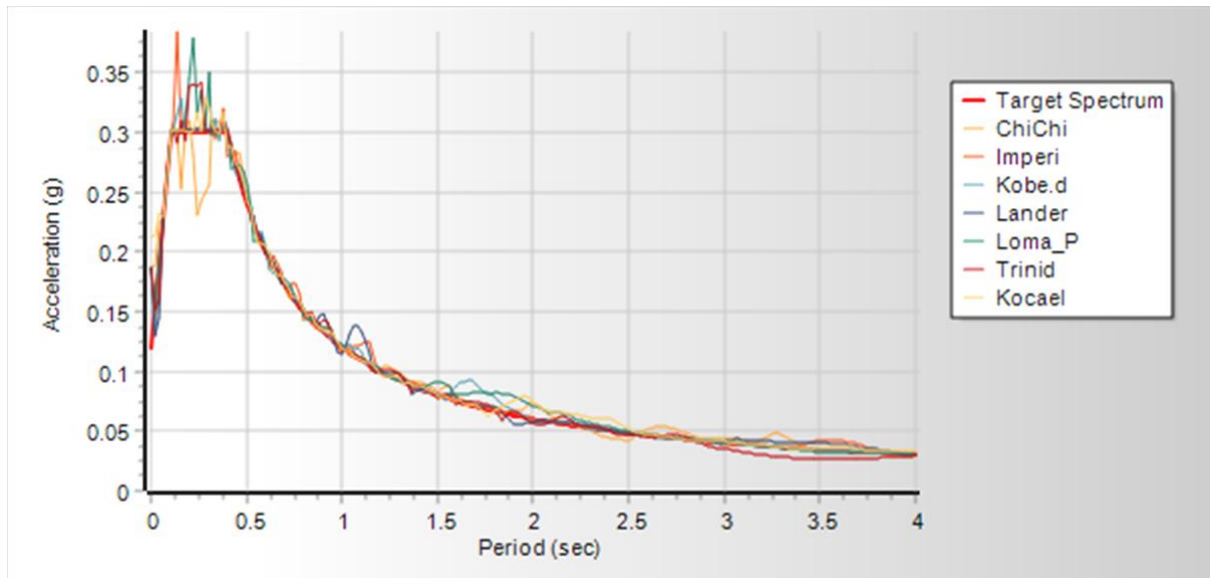


Figure 4.2b Matched earthquake accelerogram values with response spectrum

4.3 Prediction of maximum dynamic response

The matched time history of the seven earthquake accelerograms are given in the fig 4.3a. This acts as the time history input for the structure of interest. The input signals are received in the .csv format in the front panel of LabVIEW program. The slopes of the curves are interpolated to calculate the initial stiffness. The block diagram shown in the left side of the fig 4.3b and fig 4.3c processes the input data. The flow chart of the proposed program for the application of the HHT method and the Newton–Raphson method is illustrated in Fig. 4. In this study, the integration coefficients of the HHT method applied for the proposed program are $\alpha = 0$, $\gamma = 0.5$ and $\beta = 0.25$. The formulations proposed through Newmark β Method yields accurate solution for acceleration, velocity and displacement. Thus, the change of state can be obtained for chosen seven different accelerograms. In the nonlinear moment rotation relationship, the initial stiffness is considered when unloading takes place.

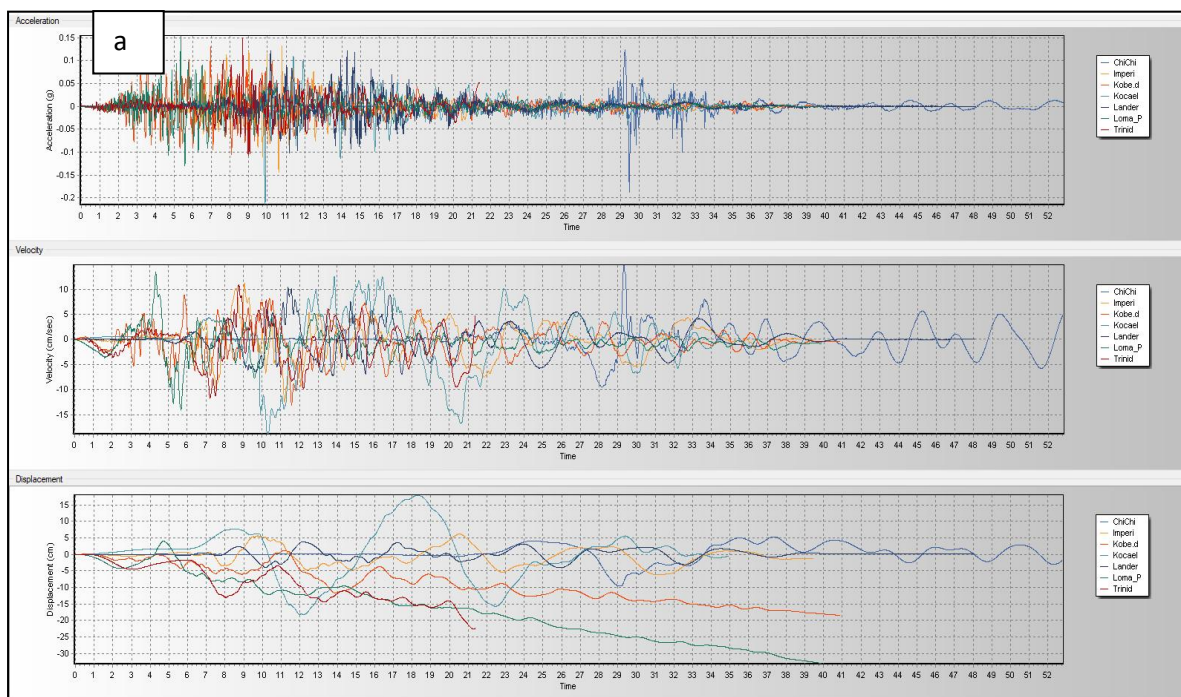


Figure 4.3a Matched time history accelerograms

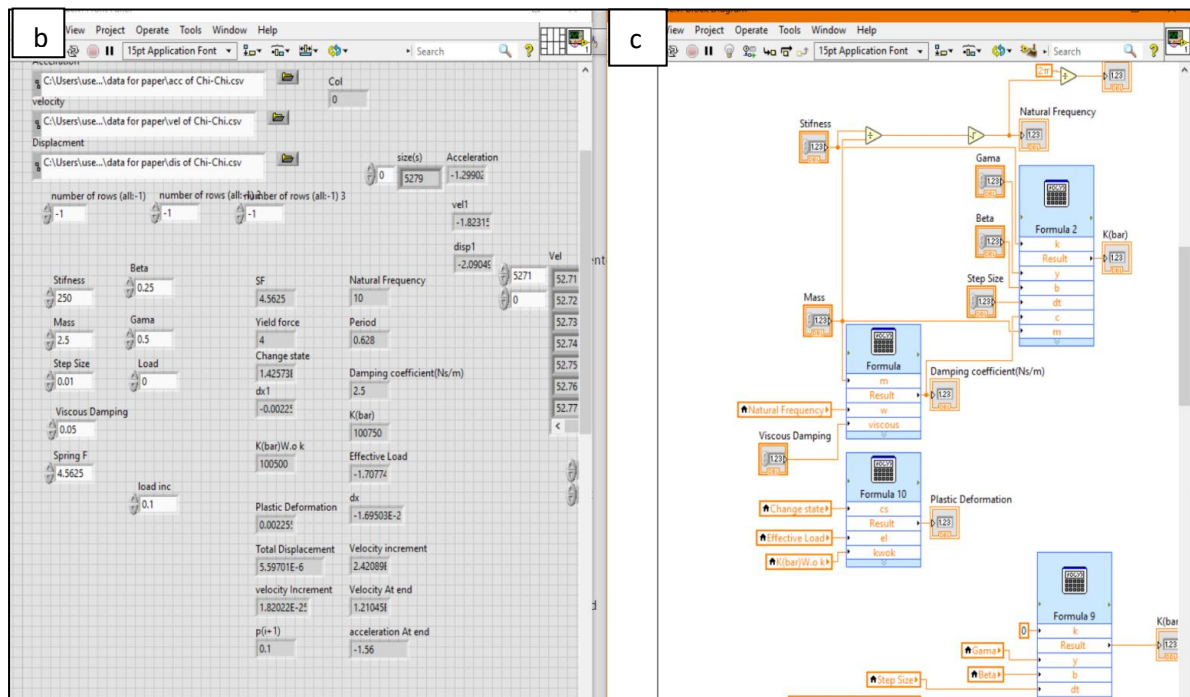


Figure 4.3b and c

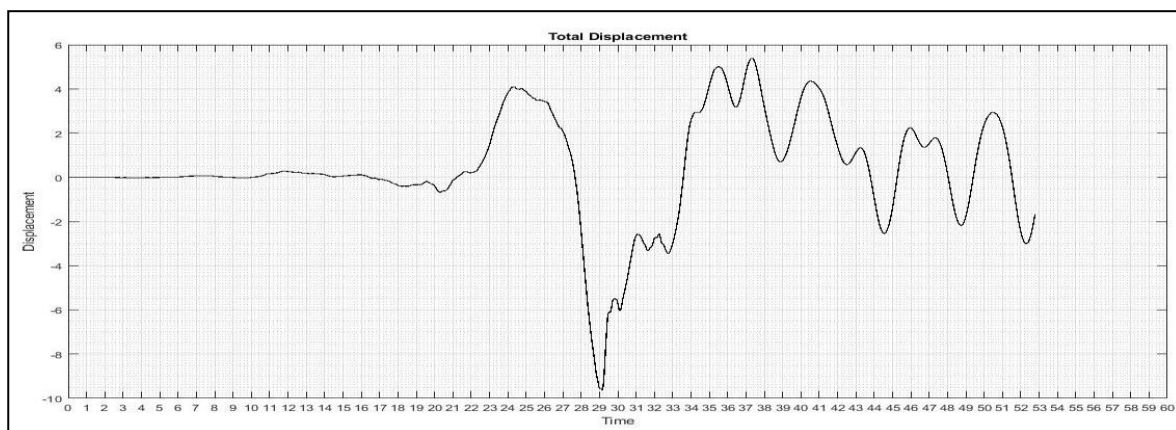


Figure 4.3d



Mode	ModFrequency [Hz]
1.	11.42
2.	29.394
3.	36.962
4.	37.627
5.	58.261
6.	60.012

It is clearly noticed from the fig 4.3d that the plastic stage with stiffening behaviour due to catenary action occurs if the level of gravity is high enough and the acceptance criteria is not exceeded. The value first decreases and then increases with increase in the vertical displacement when the catenary action in the steel is initiated. Thus the state transition is taken care by iteration procedure to minimize the unbalanced force.

V. Conclusion:

The paper proposes a time stepping procedure for nonlinear steel structure for identifying plastic hinges as an alternative to the conventional methods, as they very complex and time consuming the inelastic response of the structure is estimated from the nonlinear response history analysis of a modal inelastic single degree-of-freedom system. The accuracy of the proposed method is first validated by comparison with nonlinear time history analysis of a numerical problem and then extended to nonlinear analysis taking in account of earthquake accelerograms. The study has led to the following conclusions:

1. Applied to different case studies, the proposed procedure has revealed a good accuracy in predicting the acceleration, velocity and displacement demand when conducting a nonlinear time history analysis on the structure. Moreover, the results give a good match at a wide range of accelerogram values, until the different time steps and load increments.

2. The results obtained have highlighted that by enabling plastic analysis to find out the plastic moment M_p value of any system, there are two things that are inherently required: 1) the system should be statically indeterminate to a very high degree, 2) the junction should be checked for enough curvature ductility. It is also understood that the structure when subjected to collapse mechanism should sufficiently rotate in the joints where the plastic hinge is located, to transfer the moments to the adjacent section. Hence, determination of moment curvature ductility is more predominant in performing plastic hinge analysis.

3. It must be highlighted that the nonlinear iterative procedure for locating the control points is based on the following assumptions: 1) The material obeys Hooke's law until the stress (σ) reached the first yield value on further yielding, i.e. $\sigma = \sigma_y$ remains constant; 2) the upper and lower yield points in tension and compression are same; 3) plane section remains plane before and normal before and after bending; 4) material is homogeneous and isotropic both in elastic and plastic state; 5) there is no resulting force acting on the member; 6) the cross-section is symmetric about an axis through which the centroid passes and is parallel to the plane of bending; 7) the beam is subjected to moment and no shear is considered; 8) every layer is free to expand and contract and remain independent with respect to the adjacent layer. Nevertheless, the procedure proved to be accurate in the case studies examined in this paper, it was estimated by symmetric loop usually associated with cyclic earthquake loading. However, further developments may be useful to calibrate on the basis of experimental hysteresis response under ramp loads.

4. Finally, it must be concluded that the analysis is based on neglecting the imperfections introduced due to explicit method. The consequence of the failure of beam-column connections, the effects of tensile load transfer and their conservative nature should be considered in future studies. In spite of the aforementioned simplifying assumptions, the results observed are expected to be reproduced as a complete approach for understanding the state of transition.

Acknowledgements:

The authors would like to acknowledge the Ministry of Human Resources and Development (M.H.R.D), India and National Institute of Technology Raipur, India for all help and support.

Compliance with ethical standards

Conflict of interest:

The authors declare that they have no conflict of interest.

References:

- [1] Applied Technology Council, "ATC 40 Seismic Evaluation and Retrofit of Concrete Buildings Redwood City California," *Seism. Saf. commissionsion*, vol. 1, no. November 1996, p. 334, 1996.
- [2] FEMA, "Prestandard and Commentary for the Seismic Rehabilitation of Buildings," *Rehabil. Requisr.*, no. 1, pp. 1–518, 2000.
- [3] Fema 274, "NEHRP Commentary on the Guidelines for the Seismic Rehabilitation of Buildings," *Fed. Emerg. Manag. Agency, Washington, DC, Dev. by Appl. Technol. Counc.*, no. October, 1997.
- [4] M. Ferraioli, "Multi-mode pushover procedure for deformation demand estimates of steel moment-resisting frames," *Int. J. Steel Struct.*, vol. 17, no. 2, pp. 653–676, 2017, doi: 10.1007/s13296-017-6022-8.
- [5] P. Fajfar and M. Fischinger, "Fajfar 1998.Pdf," *Proceedings of the 9th World conference in earthquake engineering*, pp. 111–116, 1998.
- [6] ATC, "Improvement of Nonlinear Static Seismic Analysis Procedures," *FEMA 440, Fed. Emerg. Manag. Agency, Washingt. DC*, no. June, 2005.
- [7] Y. (2004). A. upper-bound pushover analysis procedure for estimating seismic demands of high-rise buildings. E. S. 26. 117-128. 10. 1016/j. engstruct. 2003. 09. 003. Jan, Tysh & Liu, Ming & Kao, "upper bound pushover analysis."
- [8] M. N. Aydinoglu, "An incremental response spectrum analysis procedure based on inelastic spectral displacements for multi-mode seismic performance evaluation," *Bull. Earthq. Eng.*, vol. 1, no. 1, pp. 3–36, 2003, doi: 10.1023/A:1024853326383.
- [9] A. K. Chopra and R. K. Goel, "A modal pushover analysis procedure to estimate seismic demands for unsymmetric-plan buildings," *Earthq. Eng. Struct. Dyn.*, vol. 33, no. 8, pp. 903–927, 2004, doi: 10.1002/eqe.380.
- [10] R. PINHO, S. ANTONIOU, C. CASAROTTI, and M. LÓPEZ, "a Displacement-Based Adaptive Pushover for Assessment of Buildings and Bridges," *Adv. Earthq. Eng. Urban Risk Reduct.*, pp. 79–94, 2006, doi: 10.1007/1-4020-4571-9_6.
- [11] E. Kalkan and S. K. Kunnath, "Adaptive modal combination procedure for nonlinear static analysis of building structures," *J. Struct. Eng.*, vol. 132, no. 11, pp. 1721–1731, 2006, doi: 10.1061/(ASCE)0733-9445(2006)132:11(1721).
- [12] K. Shakeri, M. a Shayanfar, and M. M. Asbmarz, "A Spectra-Based Multi Modal Adaptive Pushover Procedure for Seismic Assessment of Buildings," *14th World Conf. Earthq. Eng. Oct. 1217 2008 Beijing China*, 2008.
- [13] F. Khoshnoudian and M. Kiani, "Modified consecutive modal pushover procedure for seismic investigation of one-way asymmetric-plan tall buildings," *J. Earthq. Eng. Eng. Vib.*, vol. 11, no. 2, pp. 221–232, 2012, doi: 10.1007/s11803-012-0112-6.
- [14] M. Poursha, "An iterative process for pushover analysis of double unsymmetric-plan low-and medium-rise buildings under bi-directional seismic excitation," *Int. J. Civ. Eng.*, vol. 11, no. 2 A, pp. 100–114, 2013.
- [15] M. Kreslin and P. Fajfar, "The extended N2 method considering higher mode effects in both plan and elevation," *Bull. Earthq. Eng.*, vol. 10, no. 2, pp. 695–715, 2012, doi: 10.1007/s10518-011-9319-6.
- [16] M. Kreslin and P. Fajfar, "The extended N2 method taking into account higher mode effects in elevation," *Earthq. Eng. Struct. Dyn.*, vol. 40, no. 14, pp. 1571–1589, 2011, doi: doi:10.1002/eqe.1104.
- [17] J. C. Reyes and A. K. Chopra, "Modal Pushover-Based Scaling of Two Components of Ground Motion Records for Nonlinear RHA of Structures," *Earthq. Spectra*, vol. 28, no. 3, pp. 1243–1267, Aug. 2012, doi: 10.1193/1.4000069.
- [18] J. C. Reyes, A. C. Riaño, E. Kalkan, and C. M. Arango, "Extending modal pushover-based scaling procedure for nonlinear response history analysis of multi-story unsymmetric-plan buildings," *Eng. Struct.*, vol. 88, pp. 125–137, 2015, doi: 10.1016/j.engstruct.2015.01.041.
- [19] M. Poursha, F. Khoshnoudian, and A. S. Moghadam, "The extended consecutive modal pushover procedure for estimating the seismic demands of two-way unsymmetric-plan tall buildings under influence of two horizontal components of ground motions," *Soil Dyn. Earthq. Eng.*, vol. 63, pp. 162–173, 2014, doi: 10.1016/j.soildyn.2014.02.001.
- [20] M. Poursha and E. T. Samarin, "The modified and extended upper-bound (UB) pushover method for the multi-mode pushover analysis of unsymmetric-plan tall buildings," *Soil Dyn. Earthq. Eng.*, vol. 71, pp. 114–127, 2015, doi: 10.1016/j.soildyn.2015.01.012.
- [21] M. Poursha and M. A. Amini, "A single-run multi-mode pushover analysis to account for the effect of higher modes in estimating the seismic demands of tall buildings," *Bull. Earthq. Eng.*, vol. 13, no. 8, pp. 2347–2365, 2015, doi: 10.1007/s10518-014-9721-y.
- [22] M. A. Amini and M. Poursha, "Adaptive Force-Based Multimode Pushover Analysis for Seismic Evaluation of Midrise Buildings," *J. Struct. Eng. (United States)*, vol. 144, no. 8, pp. 1–12, 2018, doi: 10.1061/(ASCE)ST.1943-541X.0002070.
- [23] M. A. Amini and M. Poursha, "Prediction of the force demands of tall buildings through the enhanced pushover procedures," *Struct. Des. Tall Spec. Build.*, vol. 27, no. 17, pp. 1–12, 2018, doi: 10.1002/tal.1540.
- [24] M. Ferraioli, A. Lavino, and A. Mandara, "An adaptive capacity spectrum method for estimating seismic response of steel moment-resisting frames," *Ing. Sismica*, vol. 33, no. 1–2, pp. 47–60, 2016.
- [25] M. Ferraioli, "A modal pushdown procedure for progressive collapse analysis of steel frame structures," *J. Constr. Steel Res.*, vol. 156, pp. 227–241, 2019, doi: 10.1016/j.jcsr.2019.02.003.
- [26] E. Kosari, M. Poursha, and K. Abedi, "Seismic Evaluation of Tall Unstiffened Steel Plate Shear Wall (SPSW) Systems with Emphasis on Reversal Phenomenon in the Higher Mode Pushover Curve," *Int. J. Civ. Eng.*, vol. 17, no. 5, pp. 523–540, 2019, doi: 10.1007/s40999-018-0286-z.
- [27] Y. B. Yang, A. Chen, and S. He, "Research on nonlinear, postbuckling and elasto-plastic analyses of framed structures and curved beams," *Meccanica*, vol. 6, 2020, doi: 10.1007/s11012-020-01182-6.
- [28] P. C. Nguyen, T. T. Nguyen, Q. X. Lieu, T. T. Tran, P. T. Nguyen, and T. N. Nguyen, "Nonlinear inelastic analysis for steel frames," *Lect. Notes Civ. Eng.*, vol. 80, pp. 311–317, 2020, doi: 10.1007/978-981-15-5144-4_26.
- [29] P. C. Nguyen, N. T. N. Doan, C. Ngo-Huu, and S. E. Kim, "Nonlinear inelastic response history analysis of steel frame structures using plastic-zone method," *Thin-Walled Struct.*, vol. 85, pp. 220–233, 2014, doi: 10.1016/j.tws.2014.09.002.
- [30] N. Of, L. By, L. H. Teh, and M. J. Clarke, "U Sing B Eam E Lements," *Pfenninger Fowler's Proced. Prim. Care*, vol. 125, no. November, pp. 1328–1337, 1999.
- [31] Y. Liu, J. S. Kuang, and T. Y. P. Yuen, "Modal-based ground motion selection procedure for nonlinear response time history analysis of high-rise buildings," *Earthq. Eng. Struct. Dyn.*, vol. 49, no. 1, pp. 95–110, 2020, doi: 10.1002/eqe.3232.
- [32] ASCE, *ASCE STANDARD Loads for Buildings*. 2016.